# Xylenes Transformation over ZSM-5 Zeolite in a Fluidized-Bed Reactor

S. Al-Khattaf*, A. Iliyas and A. Al-Amer

Department of Chemical Engineering, King Fahd University of Petroleum & Minerals, Dhahran 31261, Saudi Arabia.

**Abstract**

The transformations of xylenes have been investigated over ZSM-5 zeolite using a fluidized-bed reactor. The sequence of xylenes reactivity is found to decrease as follows: p-xylene > o-xylene > m-xylene. o-Xylene transformation exhibits the highest isomerization/disproportionation (I/D) ratio, which decreases rapidly with reaction temperature. p-Xylene selectivity is found to be enhanced at lower reaction temperature. The value of m-xylene/o-xylene (M/O) ratio obtained with p-xylene conversion is higher than the equilibrium value in the initial stage of the reaction. This confirms that xylene isomerization proceeds via 1,2-methyl shifts with ZSM-5. The obtained results indicate higher isomerization selectivity as compared to disproportionation during the conversion of the three xylene isomers. A higher value of T/TMBs molar ratio than the stoichiometric value is obtained with all the three xylene reactants.

Keywords: Xylene transformation, fluidized-bed reactor, ZSM-5, isomerization, disproportionation

*Corresponding author. Tel.: +966-3-860-1429; Fax: +966-3- 860-4234
E-mail address: skhattaf@kfupm.edu.sa

## 1. Introduction

With increasing demand for p-xylene as starting materials for the manufacture of synthetic fibres (polyester), efforts are continually being directed to selectively produce p-xylene from low valued m-xylene. Unfortunately, the amount of p-xylene theoretically obtainable from these aromatic compounds is very much limited by thermodynamics. Consequently, attempts to overcome thermodynamic limitations in the transformation of xylenes have indeed constituted a great challenge to both the academic field and petrochemical industry. However, the introduction of ZSM-5 for xylene transformation process by Mobil workers in the early 1970s represented a clear technological improvement.

Since the commercialization of the above process, shape selective conversion of xylenes over ZSM-5 has been investigated in detail by several workers [1-12]. Modifications of ZSM-5 by various compounds have been employed to enhance p-xylene selectivity from xylene isomerization process [9, 12-14]. Similarly, para selectivity was improved by the selective coking of the external surface of ZSM-5 [15-19]. Jones et al. [8] demonstrated that P/O selectivity during the transformation of m-xylene can be utilized to characterize zeolite pore architecture.

Although abundant literatures have been published and numerous patents filed, on xylene transformation over different zeolites, however, in most instances, fixed-bed reactor is utilized for the reaction. Recently, Iliyas and Al-Khattaf reported a detailed kinetic [20] and selectivity study [21] of xylene transformation using the riser simulator, which is operated as a well mixed, fluidized-bed reactor on a large-pore Y-zeolite. In view of this, it is of interest to extend xylene transformation in the riser simulator to a medium-pore zeolite, such as ZSM-5. This will afford the opportunity to study the reaction under short contact time of the riser simulator.

Thus, the present study is aimed at investigating xylene transformation over ZSM-5 in a fluidized-bed reactor. The study will be focused on the effect of reaction conditions on the different xylene ratios i.e., p-xylene/o-xylene (P/O) ratio, p-xylene/m-xylene (P/M) ratio, and m-xylene/o-xylene (M/O). Also, the variation of isomerization /disproportionation (I/D) ratio and trimethylbenzenes (TMBs) distributions with changes in reaction conditions will be reported. The result obtained in the present study will be compared to that reported earlier over USY zeolite [21].

## 2. Experimental Section

### *2.1 The riser simulator*

All the experimental runs were carried out in the riser simulator. This reactor is novel bench scale equipment with internal recycle unit invented by de Lasa [22] to overcome the technical problems of the standard micro-activity test (MAT). For example, the low olefinity obtained from MAT reactor, due to its higher reaction time (> 75 s) as compared to the riser (< 15 s), non uniform coke deposition (150 mm long catalyst bed), and temperature/concentration gradient, which are eliminated by the well-mixed characteristics and intense fluidization of the riser simulator. The riser simulator is fast becoming a valuable experimental tool for reaction evaluation involving model compounds [23, 24] and also for testing and developing new fluidized catalytic cracking in vacuum gas oil cracking [25, 26].

The riser simulator consists of two outer shells, the lower section and the upper section, which allow one to load or to unload the catalyst easily, as illustrated in Fig. 1. The reactor was designed in such a way that an annular space is created between the outer portion of the basket and the inner part of the reactor shell. A metallic gasket seals the two chambers with an impeller located in the upper section. A packing gland assembly and a cooling jacket surrounding the shaft provide support for the impeller. Upon rotation of the shaft, gas is forced outward from the center of the

impeller toward the walls. This creates a lower pressure in the center region of the impeller, thus inducing flow of gas upward through the catalyst chamber from the bottom of the reactor annular region where the pressure is slightly higher. The impeller provides a fluidized bed of catalyst particles as well as intense gas mixing inside the reactor. A detailed description of various riser simulator components, sequence of injection and sampling can be found in work by Kraemer [27].

### *2.2 Materials*

The as-prepared ZSM-5 zeolite used in this work was spray-dried using kaolin as the filler and a silica sol as the binder. The resulting 60 μm catalyst particles had the following composition: 30 wt % zeolite, 50 wt % kaolin, and 20 wt % silica. The catalyst was calcined at 600$^{o}$C for 2 h.

### *2.3 Catalyst characterization*

The BET surface area was measured according to the standard procedure ASTM D-3663 using Sorptomatic 1800 Carlo Erba Strumentazione unit, Italy. The unit cell size was determined by X-ray diffraction following ASTM D-3942-80 procedure. The acid property of the catalyst was characterized by $NH_3$ temperature-programmed desorption ($NH_3$-TPD). In all the experiments, 50 mg of sample was outgassed at 400$^{o}$C for 30 min in flowing He and then cooled down to 150$^{o}$C. At that temperature, $NH_3$ was adsorbed on the sample by injecting pulses of 2 μl/pulse. The injection was repeated until the amount of $NH_3$ detected was the same for the last two injections. After the adsorption of $NH_3$ was saturated, the sample was flushed at 150$^{o}$C for 1 h with He to remove excess $NH_3$, and then the temperature was programmed at 30 $^{o}$C/min up to 1000$^{o}$C in flowing He at 30 ml/min. Flame ionization detector was used to monitor the desorbed $NH_3$.

### *2.4. Procedure*

The experimental procedure in the riser simulator may be summarized as follows; a 80 mg portion of the catalyst was weighed and loaded into the riser simulator basket. The system was

then sealed and tested for any pressure leaks by monitoring the pressure changes in the system. Furthermore, the reactor was heated to the desired reaction temperature. The vacuum box was also heated to around 250$^{o}$C and evacuated at around 0.5 psi to prevent any condensation of hydrocarbons inside the box. The heating of the riser simulator was conducted under continuous flow of inert gas (Ar), and it usually takes a few hours until thermal equilibrium is finally attained. Meanwhile, before the initial experimental run, the catalyst was activated for 15 min at 620$^{o}$C in a stream of Ar. The temperature controller was set to the desired reaction temperature, and in the same manner, the timer was adjusted to the desired reaction time. At this point the GC is started and set to the desired conditions.

Once the reactor and the gas chromatograph have reached the desired operating conditions, the feedstock was injected directly into the reactor via a loaded syringe. After the reaction, the four-port valve immediately opens, ensuring that the reaction was terminated and the entire product stream sent online to the analytical equipment via a preheated vacuum box chamber.

### *2.5 Analysis*

The riser simulator operates in conjunction with a series of sampling valves that allow, following a predetermined sequence, one to inject reactants and withdraw products in short periods of time. The products were analyzed in an Agilent 6890N gas chromatograph with a flame ionization detector and a capillary column INNOWAX, 60-m cross-linked methyl silicone with an internal diameter of 0.32 mm.

## 3 Results and Discussion

### *3.1 Catalyst characterization*

Zeolite catalysts for use in fluidized-bed reactor are often incorporated in amorphous matrix to achieve the desired fluidization of the catalyst particles. As a result, the determination of the

crystallinity and phase purity of the zeolite samples in the presence of this matrix is important in catalytic reactions. The XRD patterns of the ZSM-5 catalysts obtained are in agreements with those reported in the literature, without the presence of extraneous peaks. The amount of desorbed $NH_3$ (total acidity) is 0.14 mmol/g and the measured BET surface area is 70 $m^2/g$.

### *3.2 Products distribution*

The products of the transformations of the three xylene isomers are shown in Tables 1-3. As shown in these tables, the major reaction products of each xylene reactants are: the other two xylene isomers, trimethylbenzenes and toluene. The conversion obtained with each xylene is compared in Fig. 2 at 450$^o$C. It can be seen from this figure that p-xylene converts to other products more rapidly than the other two xylene isomers. Also, the conversion of o-xylene can be seen to be higher than m-xylene at all reaction temperatures and times studied. The latter results are in marked contrast to the results obtained with USY zeolite, reported by Iliyas and Al-Khattaf [20,21] under similar experimental conditions. The reactivity of the xylenes over USY zeolite was found to decrease in the following sequence: p-xylene > m-xylene > o-xylene.

In order to explain the trend in the sequence of reactivity of the xylenes over ZSM-5 used in this study, and USY zeolite in our previous study, the difference in the diffusion and adsorption of the xylene isomers over both catalysts have to be considered. With ZSM-5 zeolite, the decrease in the reactivity of the xylenes: p-xylene > o-xylene > m-xylene, demonstrates diffusional discrimination between the xylene reactants (reactant selectivity). Indeed, it has been established that the ratio of diffusion coefficient for *p* : *o* : *m* is 1000 : 10 : 1, respectively [11, 28]. As a result, p-xylene with the smallest molecular diameter diffuses faster inside the pore of ZSM-5, and thus is more accessible to the active sites as compared to the bulkier o- and m-xylenes. Furthermore, Mirth et al. [11] has reported that pronounced difference exits in the adsorption rate and surface

coverage of xylenes under non steady state conditions (similar to the condition of this study). With p-xylene reactant, adsorption-desorption equilibrium was achieved within a few seconds, while it was achieved within a few minutes with o-xylene and after 5 min for m-xylene reactant at 300$^{o}$C. This results in consistent with the basicity of the xylene isomers, which is higher for m- and o-xylene [29]. It has also been reported that the percentage coverage of Brönsted acid site for the xylenes decreases as follow: p-xylene > o-xylene > m-xylene [11]. These results perfectly explain the observed trend in the reactivity of the xylenes obtained in the present study. Thus, it is clear that the transformation of xylenes over ZSM-5 zeolite is in the transition regime of diffusion and reaction.

On the other hand, the transformation of xylenes over large pore zeolite, such as USY zeolite proceeds with little difference in adsorption and diffusion [30]. As such, the observed trend in the reactivity of xylenes over this catalyst could be due to the ease of protonation of carbon positions on the aromatic rings of the xylenes. With o-xylene reactant, the close proximity of both methyl groups results in a pronounced steric hindrance leading to the difficulty of a proton accessing the $C_2$ atom during intramolecular isomerization reaction. Consequently, o-xylene is the least reactive of the three isomers. On the other hand, m-xylene with a framework carbon between the two methyl groups has less effect of steric hindrance, while with p-xylene, the preferred protonation of the most accessible $C_4$ atom makes it most reactive [21].

The effect of temperature on the conversion of each xylene reactant is investigated at constant reaction time of 7 s as shown in Fig. 3. As expected, conversion increases with increasing temperature for the three xylene reactants. With m- and o-xylene reactants, conversion increases rapidly at lower temperature and approaches a plateau level beyond 400$^{o}$C. This indicates

secondary transformation of both xylene reactants. On the other hand, p-xylene conversion increases linearly with temperature.

### *3.3 Isomerization to disproportionation (I/D) selectivity*

The transformation of xylenes proceeds via two major reaction pathways over zeolite catalysts: isomerization and disproportionation pathways. Disproportionation reaction requires two molecules of xylene reactants with bulky transition state intermediates. As a result, disproportionation is significant on large pore zeolites that can accommodate these intermediates. However, in ZSM-5 zeolites with a smaller pore size, it is difficult to form the intermediates of disproportionation pathway (restricted transition state selectivity). Therefore, xylene transformation over ZSM-5 zeolite is generally considered to advance via unimolecular isomerization pathway with intramolecular 1,2-methyl shifts. The result of the present study supports this reaction scheme, as discussed later.

The effect of temperature on I/D ratio is shown in Fig. 4. It can be noticed that I/D ratio decreases with reaction temperature with all the three xylene reactants. This observation is inline with the fact that disproportionation requires a higher energy of activation as compared to isomerization reaction [31]. Moreover, o-xylene exhibits the highest I/D ratio at all reaction temperatures studied, although, the ratio decreases rapidly from 3.8 to 1.2 at 350 and 500$^{o}$C respectively. The higher initial values of I/D ratios with o-xylene transformation could be due to the difficulties in accommodating two molecules of the bulky o-xylene within the narrow pore of ZSM-5 zeolite during disproportionation reaction.

I/D ratio during m-xylene transformation have been utilized as a tool to characterize the zeolite pore system. However, as mentioned by Jones et al. [8], I/D ratio is not as useful in this regard as compared to P/O ratio and TMBs distribution. Nevertheless, the results presented in Fig. 5 clearly

reflect the difference in the pore size of ZSM-5 and USY catalysts, under similar reaction conditions. Whatever the xylene reactant, I/D ratio obtained over ZSM-5 is higher than USY catalysts, thus, confirming the difficulty of disproportionation route with the narrow pore of ZSM-5, as compared to USY catalyst. Furthermore, it can be noticed that the difference between I/D ratios over both catalysts, in general decreases in the sequence: p-xylene > o-xylene > m-xylene. This phenomenon can simply be explained by the order of reactivity of the xylene isomers, which as earlier shown, follows the same sequence.

### *3.4 Effects of temperature on xylene selectivity*

Fig. 6 depicts the effect of temperature on P/O ratio (for m-xylene conversion), M/O ratio (for p-xylene conversion), and P/M ratio (for o-xylene conversion). P/O ratio can be noticed to decrease with temperature from 1.7 at 350$^{o}$C to 1.24 at 500$^{o}$C. Similarly, P/M ratio decreases slightly with temperature. This suggests that p-xylene undergoes secondary reaction through either isomerization or disproportionation faster than o- and m-xylenes, in agreement with the findings of Araujo et al. [32] over SAPO-11/ZSM-5 mixed catalyst. As a result, it can be concluded that p-xylene selectivity is favored at lower temperatures. A similar observation regarding a decrease in p-xylene selectivity at elevated temperature was also reported by Vinek and Lercher [10] during the disproportionation of toluene over a ZSM-5 catalyst. Moreover, because very low conversion is obtained below 350$^{o}$C under the condition of this study, consequently, a balance has to be maintained between obtaining a high P/O ratio (at very low conversion) and a moderate P/O ratio (at a reasonable conversion level). However, it should be emphasized that the maximum value of P/O ratio predicted from theory is about 2.7 [30]. Hence, it is suggested that other techniques, such as selective coking of the external surface of ZSM-5, could be employed to increase P/O ratio, while taking advantage of the short reaction time of the riser simulator.

On the other hand, M/O ratio decreases more rapidly with temperature as compared to P/O and P/M ratios, possibly because of the conversion of m- to o-xylene at higher temperature. This interpretation can easily be understood assuming that using p-xylene as reactant, the reaction proceeds via 1,2-methyl shifts with m-xylene as the primary product, and subsequently converts to o-xylene. However, it should be mentioned that this result differs from that obtained over USY zeolite, in which there appears to be apparent direct interconversion between p- and o-xylene [20,21].

The P/O, M/O, and P/M ratios obtained in this study are compared with the thermodynamic equilibrium ratios as shown in Table 4. It can be seen that the obtained P/O ratio in this work is around 50% and 30% higher than the thermodynamic ratio at 350 and 500$^{o}$C respectively. This is indicative of enhanced p-xylene selectivity with the ten-membered ring ZSM-5 zeolite. In addition, it is interesting to observe that M/O ratio obtained in this work is about 1.8 and 1.3 times greater than the equilibrium ratios at 350 and 500$^{o}$C, respectively. This suggests that adsorbed m-xylene intermediate desorbs before a second methyl shifts to o-xylene occurs during p-xylene conversion, under the condition of this study. This is further substantiated by o-xylene selectivity plot shown in Fig. 7A, which can be seen to be zero below 2% p-xylene conversion; however, it increases afterwards with conversion. In contrast, the selectivities of m-xylene from p- and o-xylenes are closely identical at all conversion levels (Fig. 7B). Furthermore, P/M ratio is higher the than equilibrium value particularly at 350$^{o}$C, because p-xylene diffuses through ZSM-5 pores much faster than m-xylene.

The selectivity of xylene isomers obtained using ZSM-5 and USY catalysts are compared at 450$^{o}$C as presented in Fig. 8. The higher value of P/O ratio (Fig. 8A) obtained with ZSM-5 as compared to USY is quite in agreement with the monomolecular non-shape-selective

transformation process expected from the shape and size of ZSM-5. Likewise, the lower value of the M/O ratio (Fig. 8B) with ZSM-5 in comparison USY showed that o-xylene diffusivity is higher than m-xylene over the former. Similarly, the higher P/M ratio obtained during o-xylene isomerization with ZSM-5 catalysts (Fig. 8C) is also clearly indicative of the much higher p-xylene diffusivity as compared to m-xylene.

### *3.5 Trimethylbenzene distributions*

The distribution of trimethylbenzenes could be used as additional indicator of shape selectivity of zeolites. Large pore zeolites tend to have a distribution that approaches thermodynamic equilibrium [33], because the disproportionation mechanism is controlled by kinetics, rather than by thermodynamics over these zeolites [34]. On the other hand, with medium pore zeolite, such as ZSM-5 used in this study, pore diffusion has been reported to be the dominant factor influencing the distribution of TMBs [34]. Following this, it is expected that 1,2,4-TMB should be a primary product of all the three xylene disproportionation, because it has the smallest molecular diameter. However, as shown in Fig. 9, 1,2,4-TMB did not extrapolate to zero conversion, thus appearing as a secondary product during the transformation of the three xylene isomers. This is supportive of the well-established fact that disproportionation with bulky reaction intermediates is suppressed in the pore channel of ZSM-5. However, as conversion increases disproportionation increases because of the transformation of xylenes on the active sites located in the external surface of ZSM-5. The foregoing hypothesis is further substantiated by isomerization and disproportionation selectivity plot shown in Fig. 10, which depicts a higher initial selectivity of the former. A similar trend was observed for the transformation of m- and o-xylenes. In contrast, both isomerization and disproportionation have been reported to advance at similar rates during xylene transformation over USY zeolite.

Fig. 11 shows T/TMBs mole ratio at various conversion levels for each xylene reactants. As depicted in this plot, the T/TMB mole ratio obtained in this work is higher than the stoichiometric ratio of 1.0 for all the three xylenes. The higher initial value of T/TMBs mole ratio could be attributed to the slower desorption rate of trimethylbenzene isomers. A similar observation has been reported in previous studies [21,35,36]. Furthermore, the conversion of TMBs to coke molecules could also contribute to the observed behavior, because TMBs are necessary intermediates for coke formation.

**Conclusions**

The following conclusions can be drawn from transformations of the three xylene isomers over ZSM-5 in the riser simulator under the conditions of the present study:

1. The reactivity of the xylene isomers decreases in the sequence: p-xylene > o-xylene > m-xylene. This was attributed to the difference in the diffusion and adsorption capacities of the xylenes, which favors the isomers in the above sequence.
2. o-Xylene transformation exhibits the highest I/D ratio, which decreases rapidly with reaction temperature. The higher initial value of this ratio was explained by the difficulty of accommodating two molecules of the bulky o-xylene, which are necessary for disproportionation reaction within the narrow pore of ZSM-5 zeolite.
3. The decrease in P/O ratio with temperature during m-xylene transformation suggests that p-xylene selectivity is favored at lower than at higher temperature.
4. The higher value of M/O ratio than the equilibrium value, particularly in the initial stage of the reaction, confirms that xylene isomerization proceeds via 1,2-methyl shifts with ZSM-5.
5. Isomerization reaction was found to advance at a higher rate than disproportionation during the conversion of the three xylene isomers over ZSM-5.

6. The value of T/TMBs mole ratio found was higher than the stoichiometric ratio with the three xylene reactants. This was attributed to the slower desorption rate of trimethylbenzene isomers as compared to toluene.

**Acknowledgment**

The authors gratefully acknowledge King Fahd University of Petroleum & Minerals for the financial support provided for this work under the project 255. We also wish to thank Mr. Mariano Gica for his useful collaboration on the experimental work.

**References**

[1] N. Y. Chen, W. W. Kaeding, F. G. Dwyer, J. Am. Chem. Soc., 101 (1979) 6783.

[2] W. W. Kaeding, C. Chu, L. B. Weinstein, S.A Butter, J. Catal. 67 (1981) 159.

[3] W. W. Kaeding, C. Chu, L. B. Weinstein, S.A Butter, J. Catal. 69 (1981) 392.

[4] L. B. Young, S. A. Butter, W. W. Kaeding, J. Catal. 76 (1982) 418.

[5] D. H. Olson and W. O. Haag, in Catalytic materials, T. E. Whyte et al. (eds.), ACS Symp. Ser. 248, Am. Chem. Soc., Washington D.C., 1984, p. 275.

[6] V. Ducarme, J. C. Vedrine, Appl. Catal. A: Gen, 17 (1985) 175.

[7] V. S. Kayak, L. Riekert, Appl. Catal. A: Gen, 23 (1986) 403.

[8] C. W. Jones, S. I. Zones, M.E. Davis, Appl. Catal. A: Gen., 181 (1999) 289.

[9] U. Kurschner, B. Parlitz, E. Schreier, G. Ohlmann, J. Volter, Appl. Catal. A: Gen, 30 (1987) 159.

[10] H. Vinek, J. A. Lercher, J. Mol. Catal. 64 (1991) 23.

[11] G. Mirth, J. Cejka, J. A. Lercher, J. Catal. 139 (1993) 24.

[12] J. C. Vedrine, A. Auroux, P. Dejaifve, V. Ducarme, H. Hoser, S. Zhou, J. Catal. 73 (1982) 147.

[13] H. Vinek, G. Rumplmayr, J. A. Lercher, J. Catal. 115 (1989) 291.

[14] Y. Li, H. Yu, Appl. Catal. A: Gen, 142 (1996) 123.

[15] P. Ratnasamy, S. K. Pokhriyal, Appl. Catal. A: Gen, 55 (1989) 265.

[16] K. Beschmann, L. Riekert, J. Catal. 141 (1993) 548

[17] U. Kurschner, H. G. Jerschkewitz, E. Schreier, J. Volter, Appl. Catal. A: Gen, 57 (1990) 167.

[18] U. S. Pat. 4 358 395 (1982) to W.O. Haag, D. H. Olson, P. G. Rodewald.

[19] U. S. Pat. 4 508 836 (1985) to W.O. Haag, D. H. Olson, P. G. Rodewald.

[20] A. Iliyas, S.Al-Khattaf, Ind. Eng. Chem. Res., 43 (2004) 1349.

[21] A. Iliyas, S. Al-Khattaf, Accepted for publication (2004).

[22] U.S. Pat. 5 102 628 (1992) to H.I. de Lasa.

[23] S. Al-Khattaf, H.I. de Lasa, Ind. Eng. Chem. Res., 40 (2001) 5398.

[24] S. Al-Khattaf, H.I. de Lasa, Chem. Eng. Sc. 57 (2002) 4909.

[25] S. Al-Khattaf, H.I. de Lasa, Appl. Catal. A: Gen, 226 (2002) 139.

[26] S. Al-Khattaf Appl. Catal. A: Gen, 231 (2002) 293.

[27] D. W. Kraemer, Ph.D. Dissertation, University of Western Ont., London, Canada 1991.

[28] V.R. Choudhary, D. B. Akolekar, J. Mol. Catal. 60 (1990) 173.

[29] M. Seko, T. Miyake, K. Inada, The ACS/CJS Chemical Congress, Honolulu, 1979.

[30] W. Liang, S. Chen, S. Peng, Chem. Eng. Sc. 50 (1995) 2391.

[31] S. Al-Khattaf, A. Iliyas, A. Al-Amer, T. Inui, submitted for publication.

[32] A. S. Araujo, T. B. Domingos, M. J. B. Souza, A. O. S. Silva, React. Kinet. Catal. Lett. 73 (2001) 283.

[33] C. W. Jones, S. I. Zones, M. E. Davis, Appl. Catal. A: Gen,181 (1999) 289.

[34] D. J. Collins, R. J. Medina, B. H. Davis, Can. J. Chem. Eng. 61 (1983) 29.

[35] S. Laforge, D. Martin, J.L Paillaud, M. Guisnet, J. Catal., 220 (2003) 92.

[36] Y Nakazaki, N. Goto, T. Inui, J. Catal., 136 (1992) 141.

[37] Y.S. Hsu, T. Lee, H.C. Hu, Ind. Eng. Chem. Res. 27 (1988) 942

[38] T. Tsai, S. Liu, I. Wang, Appl. Catal. A: Gen., 181 (1999) 355.

Table 1. Product distribution (wt %) at various reaction conditions for m-xylene transformation

| Temp ($^{o}$C)/ time (s) | m-xylene | p-xylene | o-xylene | toluene | TMB |
|---|---|---|---|---|---|
| 350 | | | | | |
| 3 | 97.7 | 0.8 | 0.6 | 0.5 | 0.5 |
| 7 | 96.9 | 1.0 | 0.8 | 0.6 | 0.7 |
| 10 | 94.2 | 2.1 | 1.4 | 1.2 | 1.2 |
| 15 | 91.8 | 3.4 | 2.0 | 1.4 | 1.5 |
| 400 | | | | | |
| 3 | 96.2 | 1.0 | 1.0 | 0.8 | 0.7 |
| 7 | 91.6 | 2.4 | 2.0 | 1.7 | 1.8 |
| 10 | 88.3 | 3.7 | 2.6 | 2.4 | 2.5 |
| 15 | 82.8 | 5.7 | 3.8 | 3.4 | 3.6 |
| 450 | | | | | |
| 3 | 95.5 | 1.2 | 1.1 | 0.9 | 0.9 |
| 7 | 89.9 | 2.7 | 2.2 | 2.3 | 2.3 |
| 10 | 86.1 | 3.9 | 3.0 | 3.1 | 3.3 |
| 15 | 80.1 | 5.3 | 4.1 | 4.7 | 4.9 |
| 500 | | | | | |
| 3 | 93.9 | 1.3 | 1.4 | 1.5 | 1.4 |
| 7 | 88.9 | 2.5 | 2.4 | 2.8 | 2.8 |
| 10 | 84.6 | 3.6 | 3.2 | 3.9 | 3.8 |
| 15 | 78.0 | 5.2 | 4.4 | 5.5 | 5.6 |

Table 2. Product distribution (wt %) at various reaction conditions for p-xylene transformation

| Temp ($^{o}$C)/ time (s) | m- xylene | p- xylene | o- xylene | toluene | TMB |
|---|---|---|---|---|---|
| 350 | | | | | |
| 3 | 1.584 | 96.462 | 0.100 | 0.478 | 0.571 |
| 7 | 4.595 | 90.223 | 1.166 | 1.872 | 1.728 |
| 10 | 5.692 | 88.055 | 1.398 | 2.284 | 2.121 |
| 15 | 8.121 | 83.314 | 1.923 | 3.156 | 2.973 |
| 400 | | | | | |
| 3 | 2.631 | 94.351 | 0.754 | 1.003 | 0.932 |
| 7 | 5.360 | 87.911 | 1.604 | 2.362 | 2.255 |
| 10 | 7.302 | 83.690 | 2.025 | 3.278 | 3.076 |
| 15 | 11.413 | 75.120 | 3.318 | 4.754 | 4.624 |
| 450 | | | | | |
| 3 | 2.928 | 92.869 | 0.968 | 1.423 | 1.355 |
| 7 | 5.623 | 86.044 | 1.891 | 2.957 | 2.826 |
| 10 | 8.068 | 79.974 | 2.764 | 4.243 | 4.044 |
| 15 | 11.024 | 73.323 | 3.741 | 5.492 | 5.359 |
| 500 | | | | | |
| 3 | 2.926 | 92.388 | 2.059 | 1.615 | 1.508 |
| 7 | 5.625 | 83.986 | 2.228 | 3.731 | 3.424 |
| 10 | 7.289 | 80.075 | 2.817 | 4.507 | 4.202 |
| 15 | 10.271 | 72.723 | 3.925 | 6.034 | 5.705 |

Table 3. Product distribution (wt %) at various reaction conditions for o-xylene transformation

| Temp ($^{o}$C)/ time (s) | m- xylene | p- xylene | o- xylene | toluene | TMB |
|---|---|---|---|---|---|
| 350 | | | | | |
| 3 | 1.025 | 0.500 | 97.747 | 0.203 | 0.218 |
| 7 | 2.040 | 1.030 | 95.580 | 0.490 | 0.562 |
| 10 | 2.995 | 1.617 | 93.727 | 0.635 | 0.732 |
| 15 | 4.043 | 2.257 | 91.748 | 0.771 | 0.900 |
| 400 | | | | | |
| 3 | 1.574 | 0.671 | 96.113 | 0.622 | 0.717 |
| 7 | 4.148 | 1.848 | 90.640 | 1.449 | 1.630 |
| 10 | 6.117 | 2.819 | 86.323 | 2.042 | 2.302 |
| 15 | 6.972 | 3.560 | 84.601 | 2.140 | 2.428 |
| 450 | | | | | |
| 3 | 2.010 | 0.857 | 94.500 | 1.091 | 1.166 |
| 7 | 4.736 | 2.096 | 87.433 | 2.490 | 2.677 |
| 10 | 6.728 | 3.000 | 83.347 | 3.031 | 3.317 |
| 15 | 9.291 | 4.241 | 77.591 | 3.934 | 4.316 |
| 500 | | | | | |
| 3 | 2.169 | 0.984 | 93.610 | 1.381 | 1.378 |
| 7 | 4.636 | 2.068 | 86.451 | 2.986 | 3.073 |
| 10 | 6.443 | 2.888 | 81.810 | 3.883 | 4.047 |
| 15 | 9.306 | 4.191 | 74.431 | 5.321 | 5.595 |

Table 4. Comparison between xylene ratios obtained in this work and the equilibrium values.

| | 350°C[a] | | 500°C[b] | |
|---|---|---|---|---|
| | equilibrium | this work[c] | equilibrium | this work[c] |
| P/O | 1.01 | 1.50 | 0.82 | 1.07 |
| M/O | 2.23 | 2.26 | 2.00 | 2.30 |
| P/M | 0.25 | 0.53 | 0.43 | 0.45 |

[a] from ref. 37
[b] from ref. 38
[c] average for each temperature

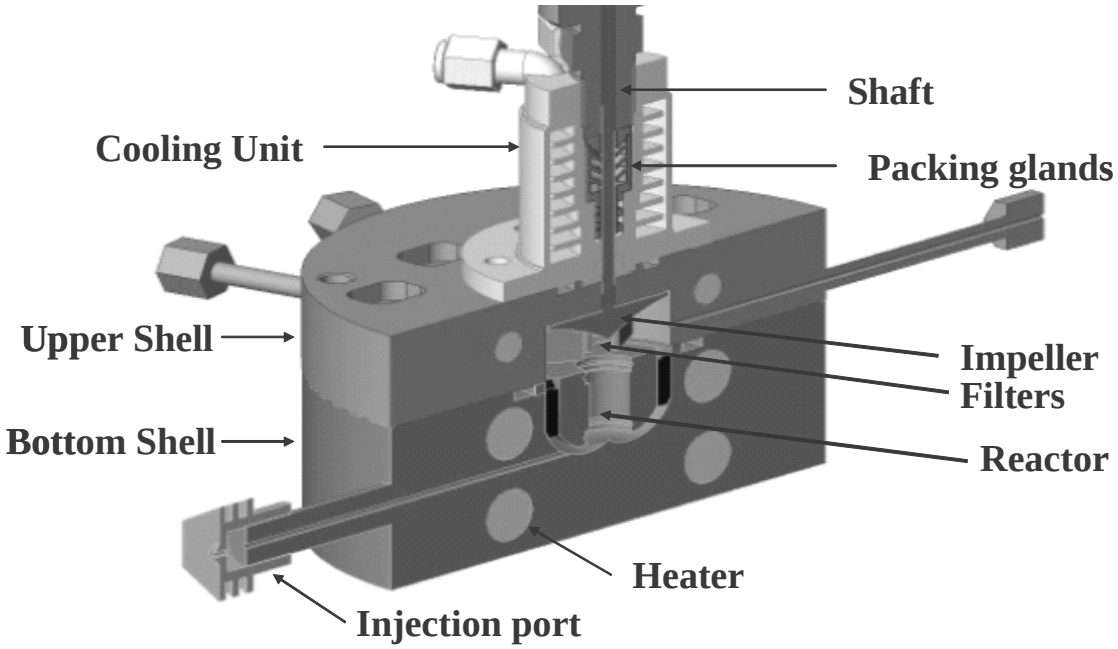


Fig. 1. Schematic diagram of the riser simulator

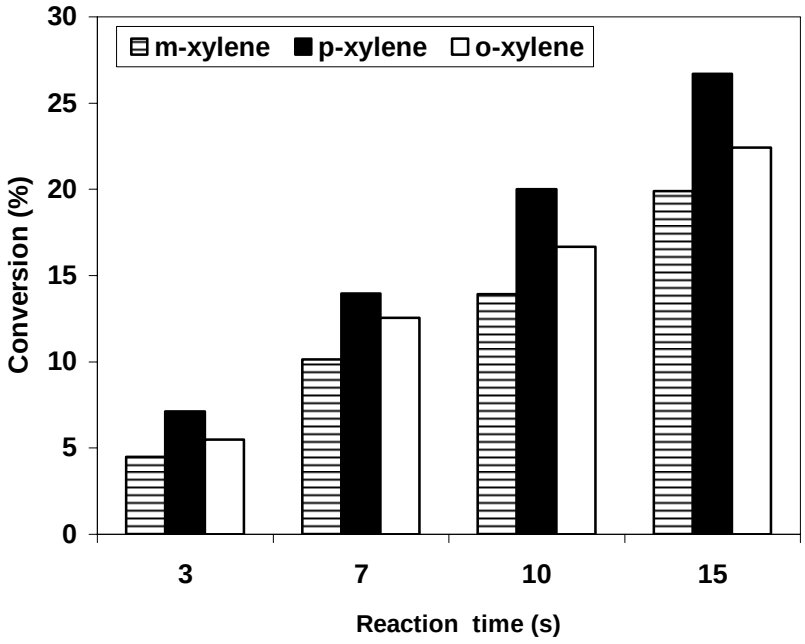


Fig. 2. Comparison between the conversions of xylene reactants at different reaction times (450$^{o}$C).

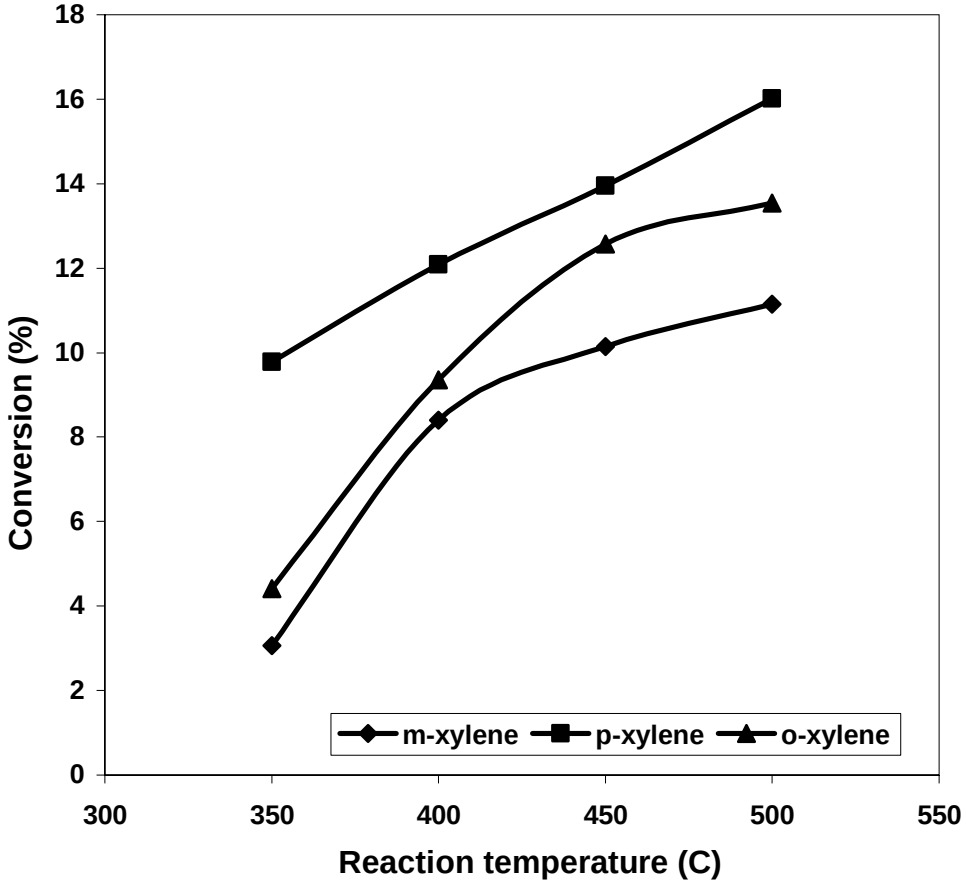


Fig. 3. Effect of reaction temperature on conversion of the xylene reactants at 7 s.

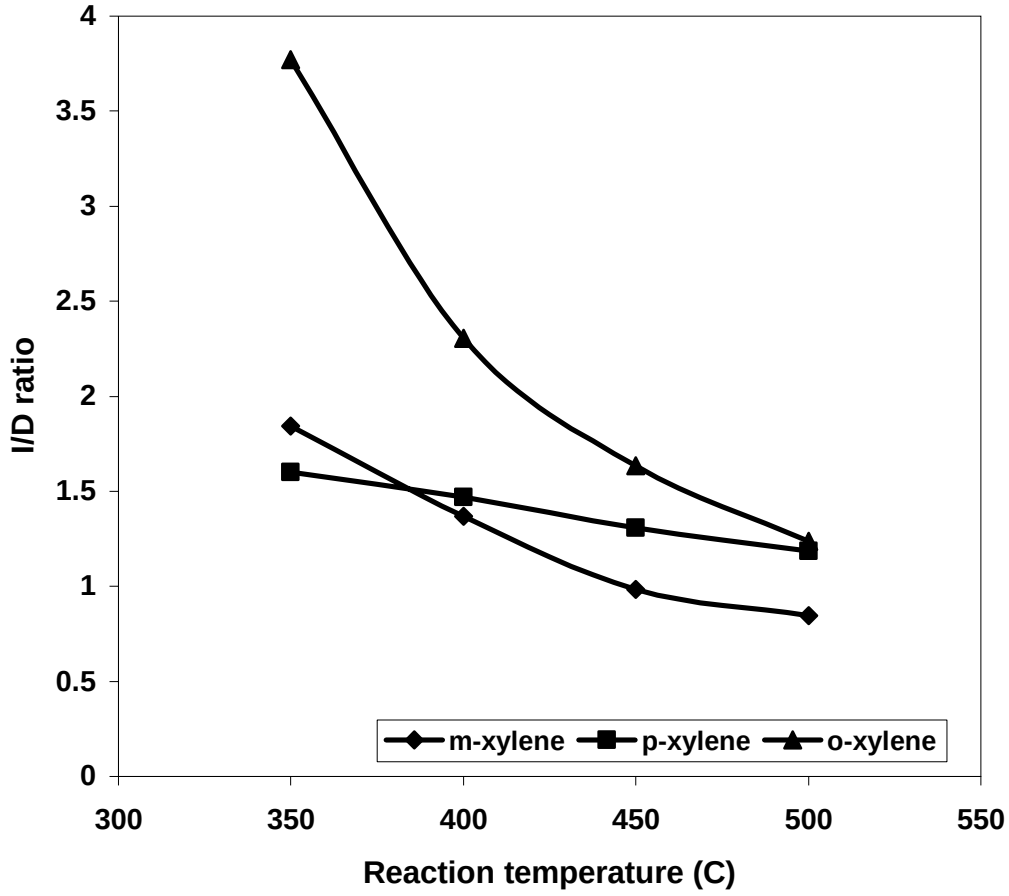


Fig. 4. Effect of temperature on isomerization/disproportionation (I/D) ratio during the transformation of each xylene isomers.

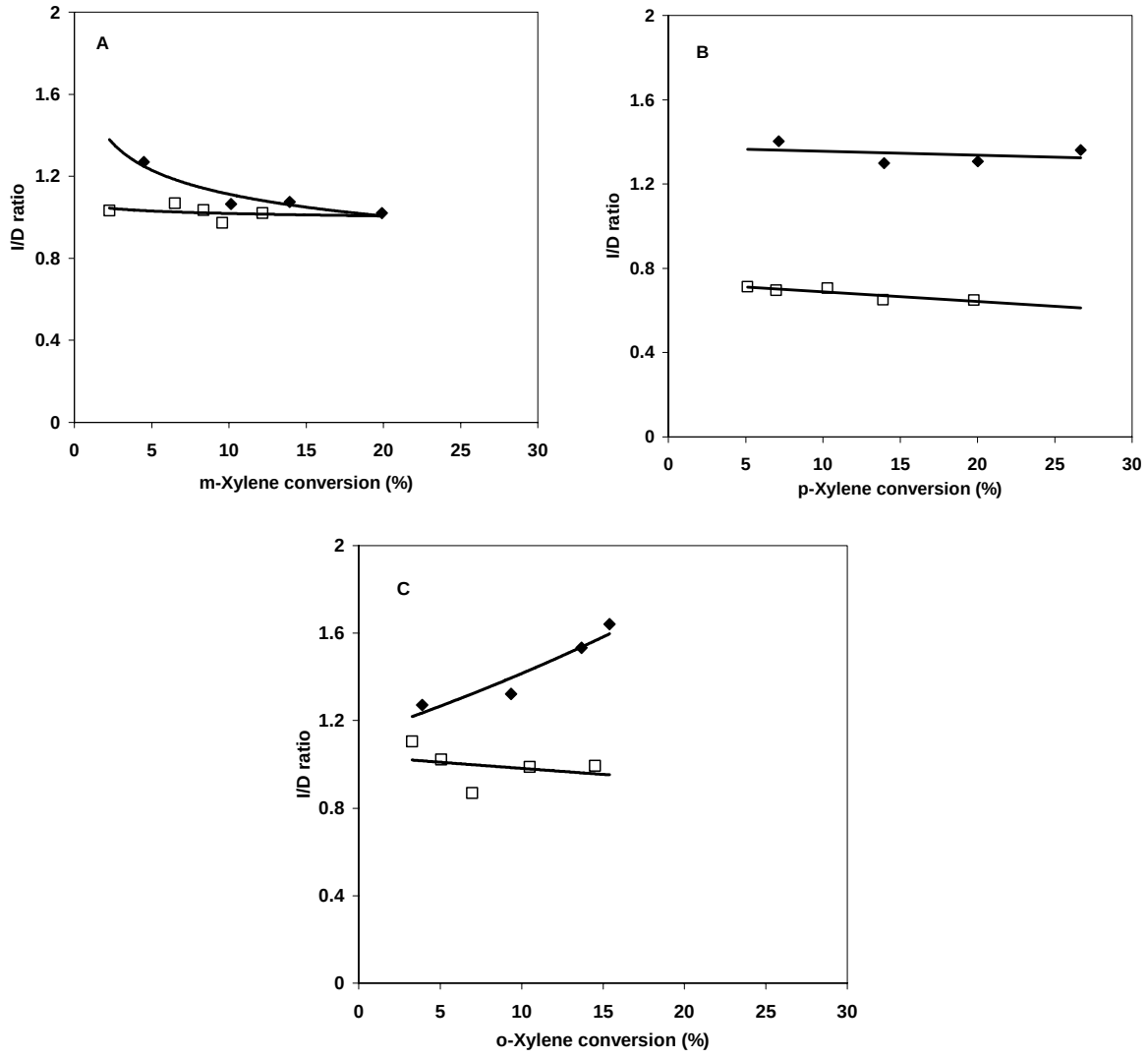


Fig. 5. Comparison between isomerization/disproportionation (I/D) ratios as function of xylene reactant conversion at 450$^{o}$C (♦) ZSM-5, (□) USY

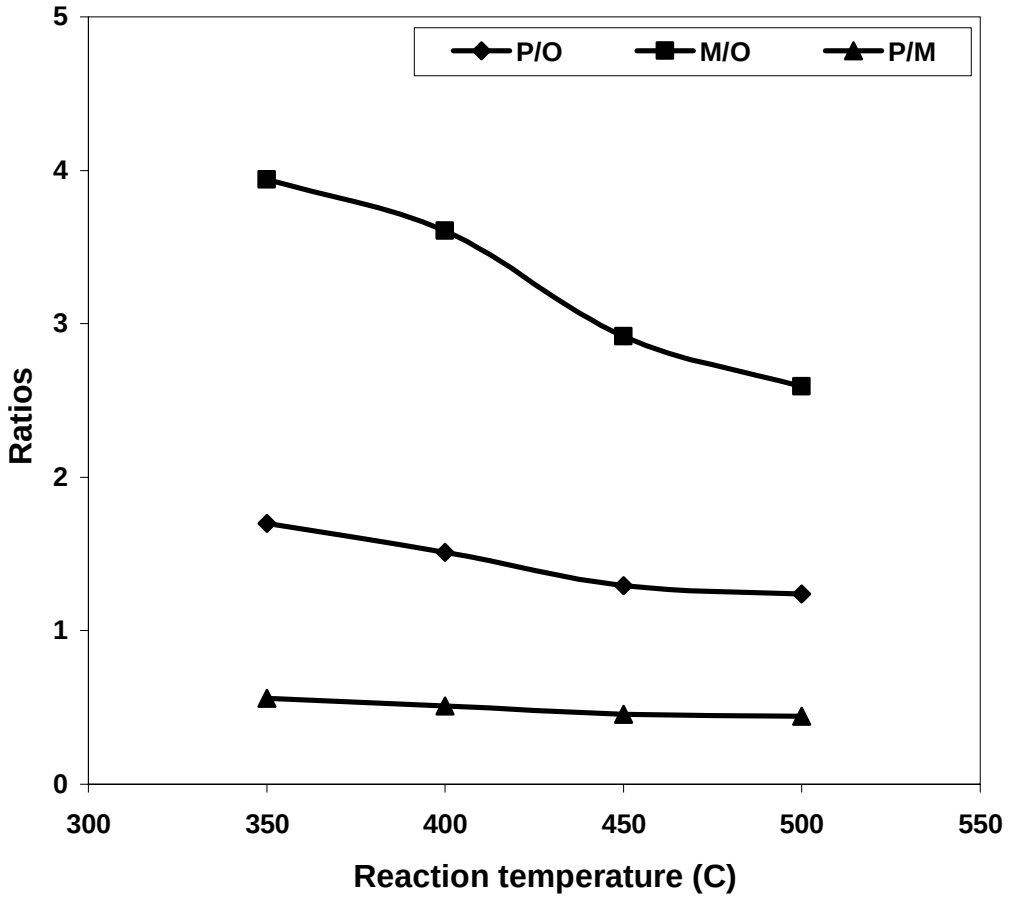


Fig. 6. Effect of temperature on xylene selectivity during the transformation of each xylene isomers.

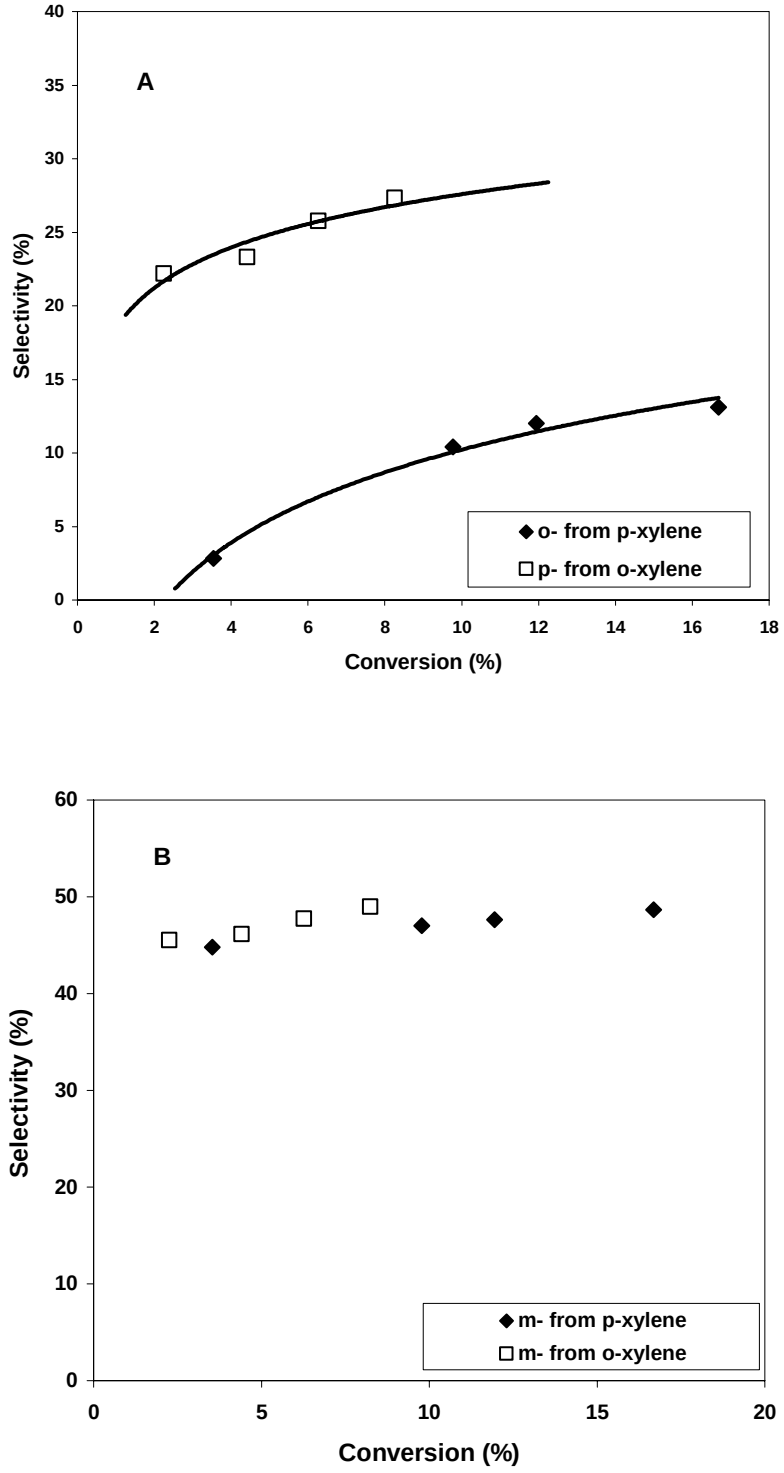


Fig. 7. Selectivity of xylenes as a function of conversion at 350$^{o}$C.

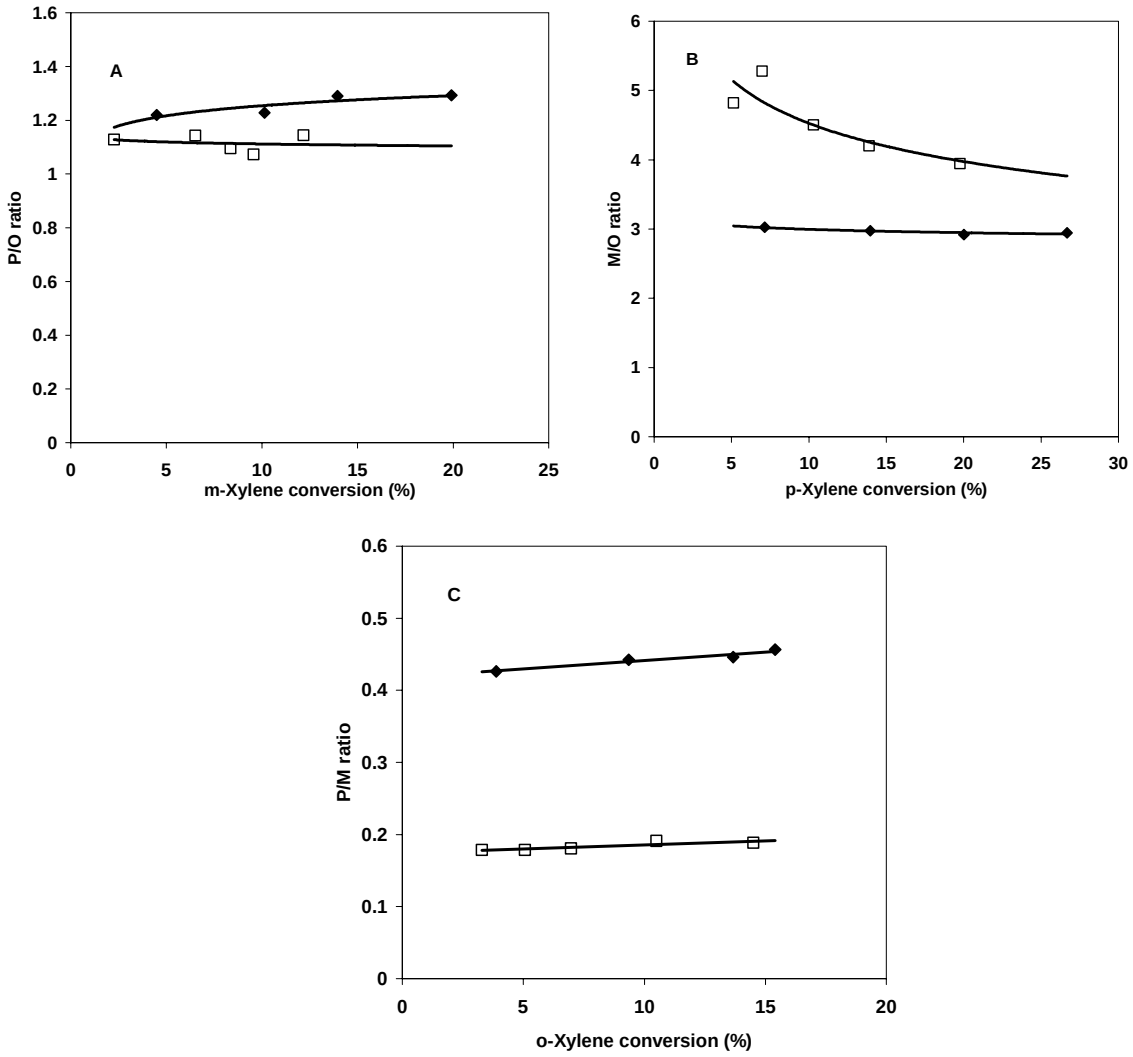


Fig. 8. Comparison between xylene selectivity as function of xylene reactant conversion at 450$^{o}$C (♦) ZSM-5, (□) USY

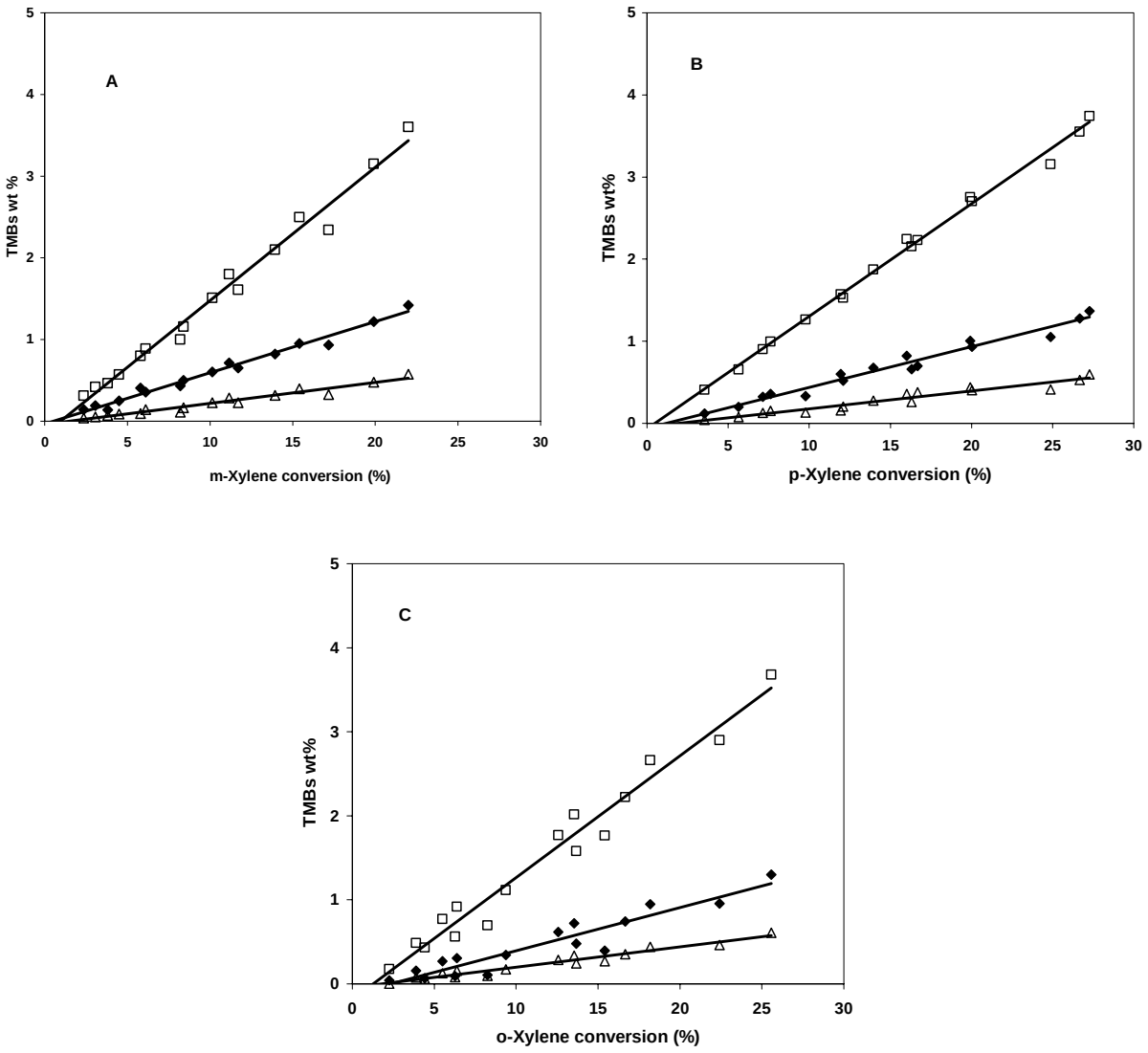


Fig.9. Distributions of trimethylbenzenes isomers as function of xylene reactant conversion. (Δ) 1,2,3-TMB, (□)1,2,4-TMB, (♦) 1,3,5- TMB

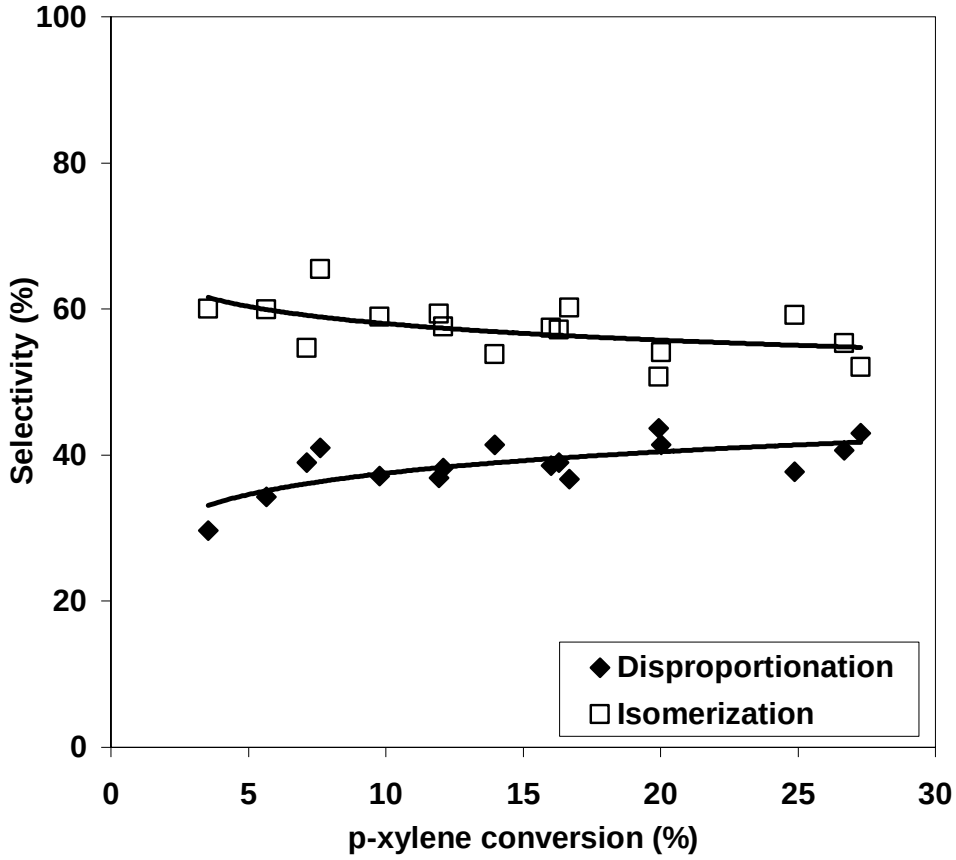


Fig. 10. Isomerization and disproportionation selectivity as a function of p-xylene conversion.

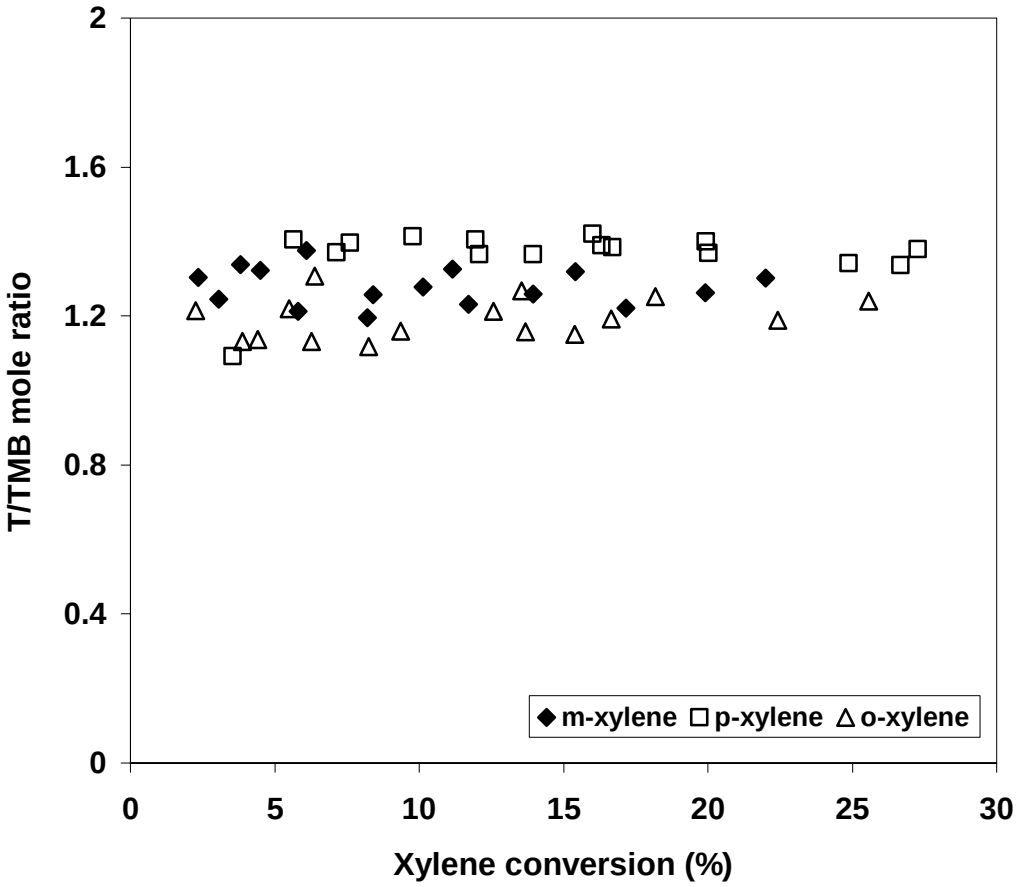


Fig. 11. Molar ratio of toluene to trimethylbenzene (T/TMBs) as a function of xylene conversion.